Möbius Dual-Mode Resonators and Bandpass Filters

Jeffrey M. Pond

Abstract—It is shown that a topological surface known as the Möbius strip has applications to electromagnetic resonators and filters. Using identical rectangles to construct a cylindrical loop and a Möbius strip results in the path length of the edge of the Möbius strip being twice the path length of an edge of the cylindrical loop. This path-length advantage is consistent with the electromagnetic analog of a Möbius strip resonating at half the resonant frequency of the electromagnetic analog of the cylindrical loop even though they have the same mean diameter.

Dual-mode Möbius resonators have been demonstrated in planar format and as wire-loaded cavities. Two-pole bandpass filters have been constructed using these resonators. It is shown that these bandpass filters possess intrinsic transmission zeros that can be adjusted to enhance filter response. An equivalent circuit, which demonstrates excellent agreement with measured data, is presented and discussed.

Index Terms—Bandpass filters, cavity resonator filters, filters, microwave filters, resonators, topology.

I. INTRODUCTION

A TECHNIQUE is presented for reducing the size of microwave resonators and filters. This technique introduces a deformation in a transmission line that is analogous to the difference between constructing a Möbius strip rather than a cylindrical loop from a rectangle. The phase change needed for resonance in these Möbius structures has contributions from the electrical length of the transmission line as well as the geometric deformation of the resonator [1]. The result is that for the same resonant frequency, the resonator circumference is reduced by a factor of two and, hence, the resonator volume is reduced by a factor of four. The validity of the concept is established with measurements of several resonators. Their practical application is demonstrated with both a planar dual-mode bandpass filter and a dual-mode wire-loaded cavity bandpass filter. Möbius resonators are shown to possess intrinsic transmission zeros, which can be exploited to realize improved bandpass filter response.

A practical definition [2] of a Möbius strip is "a one-sided surface that is constructed from a rectangle by holding one end fixed, rotating the opposite end through 180°, and applying it to the first end." The Möbius strip is probably the most common geometric shape cited to illustrate topology [2], "a branch of mathematics concerned with those properties of geometric configurations which are unaltered by elastic deformations that are homeomorphisms."

Topologically, the Möbius strip traditionally has been referred to as a one-sided surface [3] that possesses one edge. Ignoring the sinusoidal patterns discussed later, Fig. 1(a) and (b)
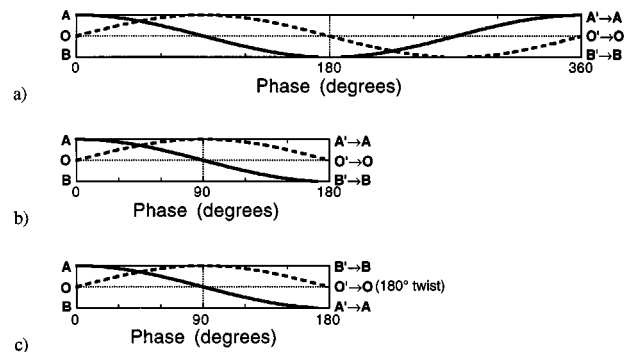
Fig. 1. When $A' \rightarrow A$ and $B' \rightarrow B$, the rectangles become (a) and (b) cylinders and (c) a Möbius strip. The length of either of the two edges (A-A' or B-B') of the cylinder formed in (a) is equal to the length of the single edge (A-B'-B-A') of the Möbius strip formed in (c). As representations of transmission lines, the two orthogonal modes (solid and dashed lines) are (a) at resonance for a "ring-type" resonator, (b) at antiresonance for a "half-length" ring, and (c) at resonance for a "half-length" ring with a 180° "twist" (Möbius resonator).

illustrates the construction of cylinders from long rectangles, while Fig. 1(c) illustrates the realization of a Möbius strip from a long rectangle. The cylinders resulting from Fig. 1(a) and (b) when A' connects to A and B' connects to B each contain two edges, A-A' and B-B'. In contrast, the Möbius strip created from Fig. 1(c) when A' connects to A and B' connects to B possesses only one edge, A-B'-B-A'. Although the length of the rectangles used to construct the cylinder in Fig. 1(a) is twice that of the edge of the rectangle used to construct the Möbius strip in Fig. 1(c), the length of the edge (A-B'-B-A') of the Möbius strip is equal to the length of the edges of the cylinder. Although synonymous with a one-sided surface, modern topology uses the term *nonorientable* (unorientable) surface to refer to the fact that globally left and right are nonsensical [4].

With the exception of certain hybrid ring or "rat-race" type structures [5]–[9], the concept of twisting the geometry to increase the total phase shift has not been widely applied to distributed electromagnetic circuits. There are several equally valid perspectives from which the existence of the resonance in a reduced volume can be viewed.

1) The path length of the edge of a Möbius strip is equal to twice the path length of O-O' in Fig. 1(c), which is 4π times the mean radius of a smoothly curved Möbius strip. This periodicity allows a resonance condition to exist in a smaller volume than can be realized without the twist.

2) Since globally left and right are nonsensical on a nonorientable surface, there appears to be a periodic alternation between left and right as the center circle (O-O' in Fig. 1(c)) of a Möbius strip is traversed. Similarly, a traveling wave on a transmission line experiences periodic reversals in polarity. By projecting a transmission line onto

a nonorientable surface and phasing the electromagnetic oscillation with the path length associated with reversal of left and right (the path length of **O**-**O**′ in Fig. 1(c)), a resonant condition occurs.

3) Since the Möbius strip contains a 180° twist, the distributed electromagnetic analog is expected to require a "circumference" (the path length of **O**-**O**′ in Fig. 1(c)) corresponding to a half-wavelength. When combined with the 180° twist, a total phase change of 360° occurs and a resonant condition results.

II. CONCEPTS

A Möbius resonator possesses several properties that can be useful in realizing filters. Prior to presenting experimental results, it is appropriate to discuss several important concepts, including the existence of two degenerate orthogonal modes [10] and the origins of intrinsic transmission zeros. Also discussed are generalized Möbius-type geometries that have the potential to offer even more compact resonators and filters.

A. Dual-Mode Resonance

Fig. 1 graphically demonstrates the existence of two degenerate orthogonal modes. Fig. 1(a) shows the sinusoidal (dashed line) and cosinusoidal (solid line) pattern of a wavelength of a signal on a transmission line. The horizontal axis, labeled in degrees, is proportional to the length. If this length of the transmission line is smoothly bent around on itself such that **A** connects to **A**′ and **B** connects to **B**′, then both the sinusoidal and cosinusoidal patterns and their derivatives match and they represent the two degenerate orthogonal modes of a "ring resonator type" resonance.

In contrast, in Fig. 1(b), the length of the line is only a half-wavelength long. It is well known that if the same procedure that was applied to Fig. 1(a) is applied to Fig. 1(b), the requirements for resonance will not exist since the cosinusoidal pattern will not match. Even though the sinusoidal pattern does meet, its derivative is not continuous.

However, consider a section of transmission line that is of equal length to that shown in Fig. 1(b), and perform a twisting of the one end by 180° before applying it to the first end. As shown in Fig. 1(c), the resonance condition is met since **A** connecting to **A**′ and **B** connecting to **B**′ results in the both the sinusoidal and cosinusoidal modes and their derivatives' matching smoothly. Both Fig. 1(a) and (c) possess two degenerate modes at the same frequency, even though the volume, as illustrated in Fig. 2, occupied by Fig. 1(c) is one-fourth that occupied by Fig. 1(a).

B. Transmission Zeros

In addition to the dual-mode resonance, intrinsic transmission zeros exist when configured as a bandpass filter. Without concern for the practical aspects of realizing the filter, the diagrams in Fig. 3(a) and (b) reveal the origins of these transmission zeros assuming ideal lossless transmission lines.

The first of these transmission zeros arises from coupling into the Möbius resonator, as shown in Fig. 3(a), and can be considered to be a short circuit at the input port. With p representing
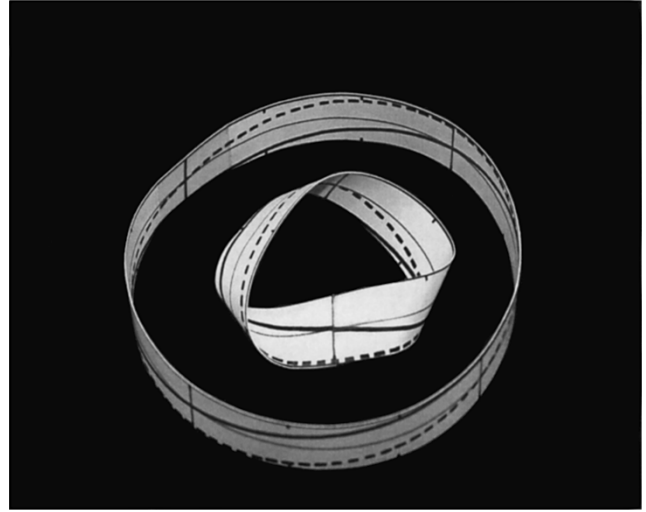

Fig. 2. Comparison of a model of a cylindrical loop resonator [from Fig. 1(a)] and a model of a Möbius strip resonator [from Fig. 1(c)] with the same resonant frequency.
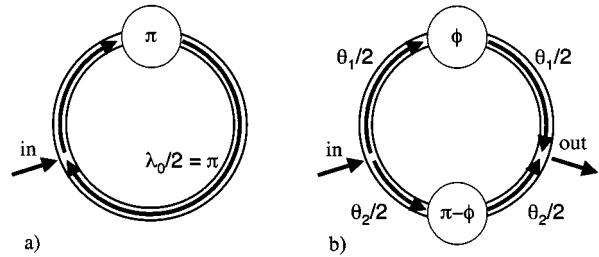

Fig. 3. Transmission zeros exist due to short circuits at the (a) input port and (b) output port. At the input port, an incident wave at the resonant frequency is (a) out of phase, with the natural mode of the resonator due to the 180° twist. If (b) configured as a bandpass filter, with ϕ and $\pi - \phi$ representing the Möbius deformation, a transmission zero appears at the output port when $\phi = (\theta_2 - \theta_1)/2$.

the 180° phase shift associated with the twist, resonance occurs when the electrical path length is a half-wavelength ($\lambda_0/2$). However, during the time the phase in the resonator has undergone a total shift of 360°, the phase of the signal on the input line has only undergone a 180° shift. As a result, the input port forcing function is out of phase with the resonant signal in the resonator. Thus, this input port short circuit is coincident with the natural resonance of the resonator. As will be demonstrated later, this does not preclude realizing useful bandpass filter characteristics.

The second transmission zero, as illustrated in Fig. 3(b), can be placed to either side of the dual-mode resonances and located at any desired frequency separation from the resonances. This transmission zero can be considered to be a short circuit at the output port. The phase shifts ϕ and $\pi - \phi$ represent the total 180° phase shift due to the twist, while the phase shifts θ_1 and θ_2 represent the phase lengths along the transmission line segments. At the fundamental Möbius resonance, $\theta_1 + \theta_2 = 180°$. Assuming the incident signal is split equally into the upper and lower arms, the two signals will arrive to be combined at the output port. When $\phi = (\theta_2 - \theta_1)/2$, the signals at the output cancel each other. If $\phi = 0$, the transmission zero exists for all

frequencies, even when $\theta_1 = \theta_2 = 90°$, which is the fundamental Möbius resonance.

These transmission zeros are intrinsic to the ideal circuit. Although similar characteristics have been seen in traditional ring resonators [11] and have been exploited to realize filters with desirable passband characteristics [12], [13], nonidealities or nonuniformities are required.

C. Higher Order Structures

In the following, terms are used without rigor since it is desired only to covey certain geometric shapes rather than describe them with mathematical precision. A generalized "Möbius-type" structure can be realized by using an "annulus," where the annulus cross section has an n-fold ($n = 2$) rotational symmetry. As the cross section is rotated around the center of the annulus, the rotation of the cross section about its center must be $m * (360°/n)$, where m is an integer, if the edges and surfaces are to meet smoothly. The Möbius geometry described in Fig. 1 is the case of $m = 1$ and $n = 2$ where the annulus cross section is a line segment.

If the cross section of the annulus were two perpendicular lines segments that meet at their centers (i.e., an "X" that has four-fold rotational symmetry) and $m = 2$, the result is two Möbius strips that intersect along their center circles. The resultant surface has only two "sides" and two "edges." In contrast, for $m = 1$ and $n = 4$, the surface would have one edge and is a Möbius strip that intersects itself along its center circle. As a resonator, a four-fold reduction in circumference would result, leading to a 16-fold reduction in volume. These geometries are related to the topological study of projected planes associated with nonorientable substantial surfaces in Lens Spaces [4]. Both $m = 1$, $n = 2$ and $m = 2$, $n = 4$ exist in lens space [2,1], whereas $m = 1$, $n = 4$ exists in Lens Space [4,1]. Further discussion is beyond the scope of this paper.

Measured results on wire-loaded cavity resonators with $m = 1$, $n = 2$ and $m = 1$, $n = 4$ are presented later. Although the following nomenclature is unique to this presentation, for convenience the $m = 1$, $n = 2$ and $m = 1$, $n = 4$ geometries are referred to as 4π and 8π Möbius resonators, respectively, in reference to their periodicities.

III. PLANAR DUAL-MODE RESONATORS AND FILTERS

A two-pole bandpass filter was fabricated using a planar implementation of a dual-mode Möbius resonator. The "twist" is implemented using two via connections through the substrate, as illustrated in Fig. 4(a). The filter employs a copper-clad Teflon substrate that requires conductor patterning on both sides. The main portion of the resonator is composed of a nearly closed "C" on each side of the substrate. Since the same photolithographic mask is used to pattern both surfaces, if the backside conductor pattern could be viewed through the substrate in Fig. 4(b), it would appear to be a mirror of the pattern that can be seen. Given the phase velocity reduction due to Teflon ($v_g \approx 2.0 \times 10^{10}$ cm/s), a microstrip ring resonator with the same 3-cm mean diameter and strip width would possess a fundamental mode at approximately 2.1 GHz.
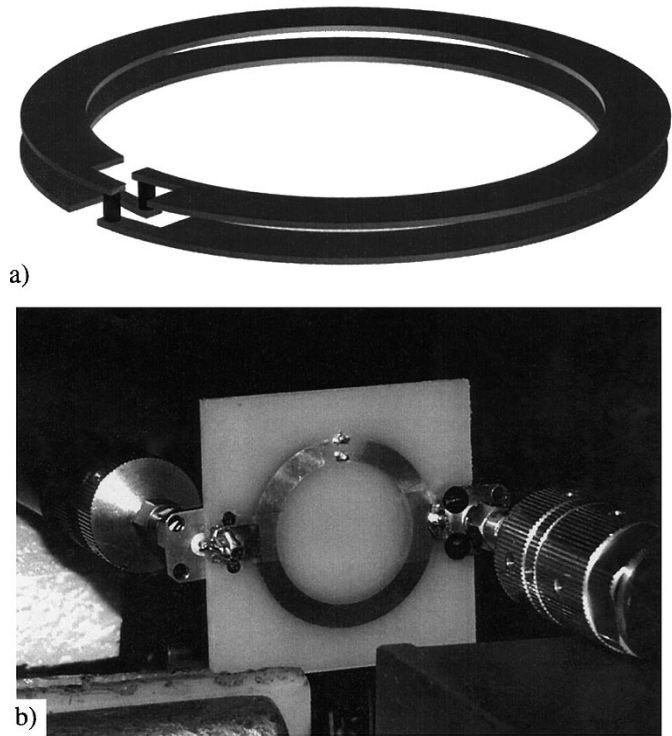

Fig. 4. (a) Drawing of a planar implementation of a Möbius resonator, where the "twist" is implemented with two vertical interconnects. (b) Photograph of a capacitively coupled planar dual-mode Möbius bandpass filter as realized on a Teflon substrate.

After patterning the metal, two via holes were drilled in the substrate. The "twist" results from inserting short wires through the vias and soldering the wires to the top and bottom conductor. This can be seen at the top of Fig. 4(b), where the vias are located at the ends of what appear to be a single interdigitated finger pair.

The very short input and output transmission lines were placed 180° apart. The "twist" was placed at 90° to the input and output lines. Both conductors of both the input and output line are capacitively coupled to the resonator. Since gap coupling could not be controlled to sufficient accuracy, a thin dielectric was deposited on the resonator so that an overlay of the input and output lines would facilitate adjusting the coupling capacitances without making dc electrical contact. The experimental results are summarized in Fig. 5, where the coupling capacitances have been adjusted empirically to obtain the results shown. As expected, the passband is centered near 1 GHz. Both modes are obvious in the reflection curve, which exhibits 16 dB of return loss. Although out-of-band performance is limited by parasitic coupling, evidence of a transmission zero can be seen just above the passband.

IV. WIRE-LOADED CAVITIES

Wire-loaded cavities were chosen as an obvious implementation of the Möbius concept. Helical wire-loaded cavities are well known for their size advantage in comparison to empty cavities [14], [15]. Although the fundamental frequency of a helical wire-loaded cavity does not possess two degenerate modes, the
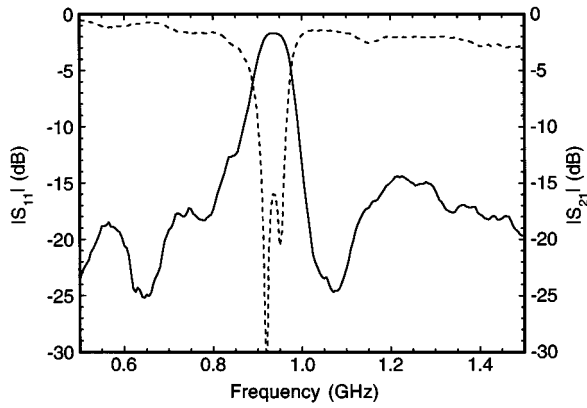
Fig. 5. The measured magnitudes of the forward transmission ($|S_{21}|$) and reflection ($|S_{11}|$) scattering parameters of the planar structure shown in Fig. 4 are given by the solid and dashed lines, respectively. The shape of the reflection parameter clearly demonstrates the dual-mode nature of the resonance.

Fig. 6. Wire structures fabricated from 0.085-in diameter coax with the outer conductor removed: a 4π Möbius (upper left), 8π Möbius (lower left), a double loop (upper right), and a 4π helix (lower right).

TABLE I
PROPERTIES OF WIRE STRUCTURES FABRICATED FROM 0.085-in-DIAMETER COAX WITH THE OUTER CONDUCTOR REMOVED

Wire Geometry	Fundamental Resonant Frequency (GHz)	Unloaded Quality Factor (Q_u)
4π Möbius	2.124	386
8π Möbius	1.035	305
Two parallel loops	4.322	433
4π helix	0.819	304

fundamental frequency of a Möbius wire-loaded cavity is expected to possess two degenerate modes. Thus Möbius loaded cavities may possess some advantages in comparison to helix loaded cavities in the realization of wire-loaded cavity filters.

A hollow cylindrical copper cavity with a diameter of 2.5 cm and a height of 0.9 cm was used for these measurements. When empty, this cavity has a fundamental frequency at 9.04 GHz. The cavity has a single end plate that is clamped with four screws. Input and output ports were placed 180° apart in the cylindrical wall. Small coupling loop antennas, fabricated from 0.085-in-diameter coaxial cable, were used to examine the properties of the resonances. These were mounted with a clamp that allowed the strength of the coupling to be varied by sliding the loop further into the cavity. For the bandpass filter discussed later, the center conductors of the input and output coaxial cables were extended into the cavity and bent in a circumferential arc.

A. Resonators

Several wire structures were fabricated using 0.085-in diameter coaxial cable from which the outer conductor had been removed leaving the center conductor sheathed in the dielectric. As this would add some dielectric loading to the cavity, conventional wire geometries were fabricated to compare to the Möbius wire-loaded cavity. The four wire structures measured are shown in Fig. 6. Depending on the particular geometry, all of the wire structures were hand shaped from 6.1, 12.2, or 24.4 cm lengths of cable so that the mean diameter was always 1.94 cm. Small glass reinforced dielectric spacers were used to maintain a uniform wire separation.

The measured resonances of all four structures are shown in Figs. 7–10. The 4π Möbius wire, shown in the upper left of Fig. 6, when placed in the cavity results in the resonances shown in Fig. 7. A fundamental dual-mode resonance is clearly seen just above 2 GHz. Similarly, the transmission zeros are evident, with one being slightly above and the other slightly below the resonance peaks. The resonances at 4.2 and 4.5 GHz do not correspond to higher order Möbius resonaces but, rather, are determined by the fundamental even mode of a two conductor line where the cavity wall is ground. Due to the 180° phase shift induced by the twist, higher order Möbius modes, which
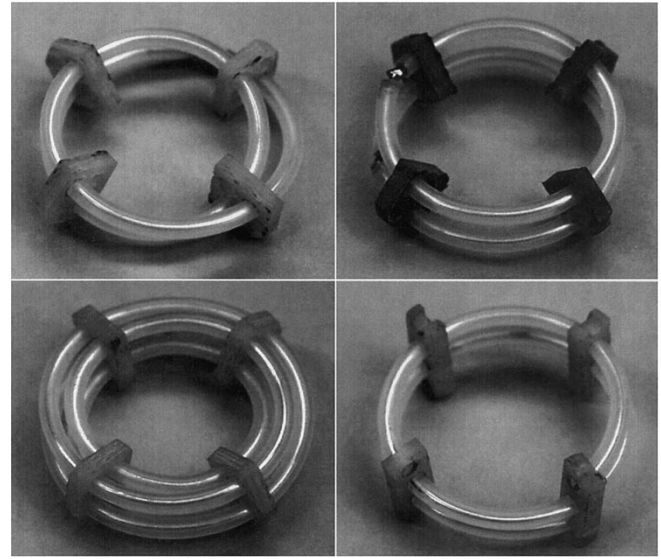
are related to the odd mode of a two conductor line, exist only when the path length corresponds to odd integer multiples of a half-wavelength.

The 8π Möbius wire, shown at the lower left of Fig. 6, when placed in the cavity results in the resonances shown in Fig. 8. A fundamental dual-mode resonance is clearly seen just above 1 GHz. As expected, this is at half the resonant frequency of the 4π Möbius resonator. Again, the transmission zeros are evident, with one being slightly above and the other slightly below the resonance peaks. A discussion off the higher order modes is beyond the scope of this paper.

For comparison purposes, it is illustrative to examine a wire structure consisting of two parallel loops, as shown at the upper right of Fig. 6. This structure is analogous to the geometry of Fig. 1(a), whereas the 4π Möbius wire is analogous to the geometry of Fig. 1(c). As shown in Fig. 9, the fundamental resonance of 4.3 GHz is at about twice the frequency of the 4π Möbius resonator. This is exactly the expected result given that the mean diameters are the same. However, a more careful examination reveals more than just the two modes represented in Fig. 1(a). Since the parallel loops are contained within the cavity, there
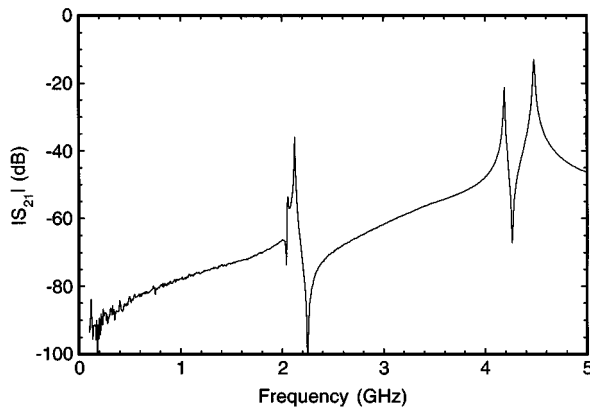
Fig. 7. The measured resonances of the dual-mode 4π Möbius wire-loaded cavity using the wire structure shown at the upper left in Fig. 6. The center frequency and Q_u of the dominant mode are given in Table I.
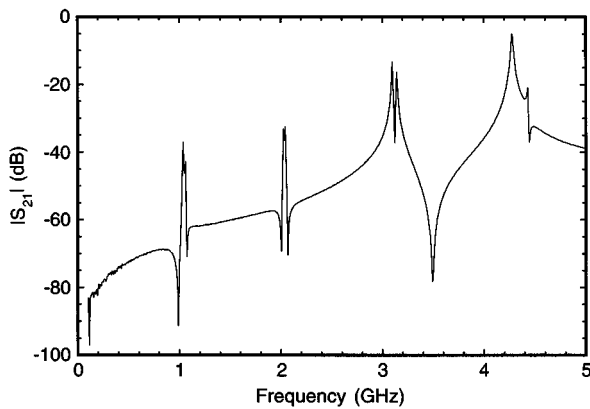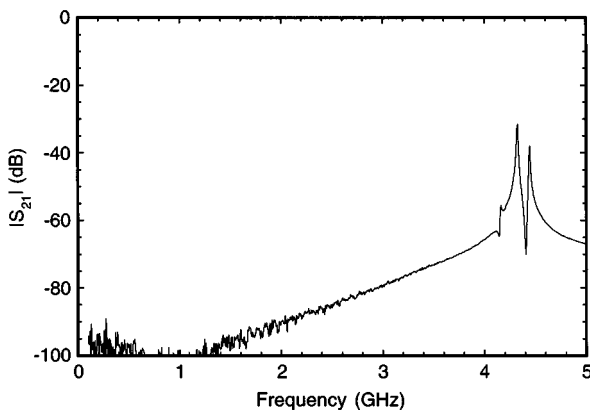

Fig. 8. The measured resonances of the dual-mode 8π Möbius wire-loaded cavity using the wire structure shown at the lower left in Fig. 6. The center frequency and Q_u of the dominant mode are given in Table I.

Fig. 9. The measured resonances of the double-loop wire-loaded cavity using the wire structure shown at the upper right in Fig. 6. The center frequency and Q_u of the dominant mode are given in Table I.

exists both $\sin(\theta)$ and $\cos(\theta)$ odd modes, as well as $\sin(\theta)$ and $\cos(\theta)$ even modes. All four of these modes, given the small fractional volume occupied by the Teflon surrounding the wires, will resonate at nearly the same frequency.

An additional wire-loading geometry, a two-turn (4π) helix, was fabricated and tested for comparison purposes. The 4π
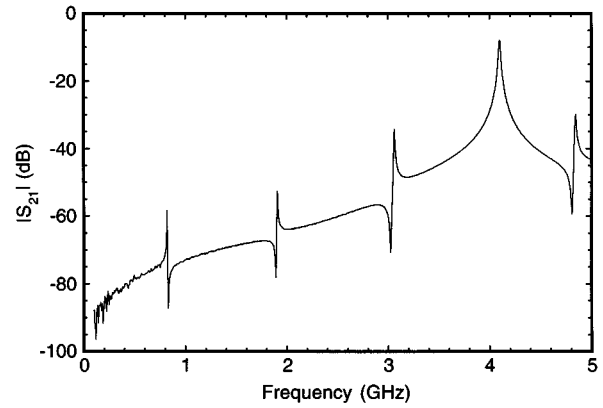

Fig. 10. The measured resonances of the 4π helix wire-loaded cavity using the wire structure shown at the lower right in Fig. 6. The center frequency and Q_u of the dominant mode are given in Table I.

helix, shown at the lower right of Fig. 6, was chosen because helical loading of cavities has been extensively studied [14], [15] and can provide a useful experimental benchmark to compare the measured resonant frequencies and quality factors. The measured results for the 4π helix are shown in Fig. 10. In terms of overall size reduction, the 4π helix resonator and 8π Möbius resonator are an interesting comparison. The 4π helix has a fundamental frequency that is about 20% lower than the 8π Möbius resonator due to the nature of the mode on the helix and the capacitive loading of the wire ends. The measured unloaded Qs of both these resonators are nearly identical. In comparison to an approximately similar size and performance helix, the primary advantage of the 8π Möbius structure is the existence of the dual-mode resonance and the transmission zeros.

B. Dual-Mode Bandpass Filter

The 4π Möbius wire fabricated from 0.085-in-diameter coaxial cable was selected to implement a two-pole bandpass filter using the dual-mode fundamental resonance. As the existing cavity had no provision for tuning screws, the only control available over the shape of the filter transfer function was the rotational position of the 4π Möbius wire in the cavity and the adjustment of the input and output port coupling antennas. Further complicating the tuning procedure was the fact that these parameters could only be varied with the top plate of the cavity removed, as shown in Fig. 11.

The measured performance of the 4π Möbius wire-loaded cavity filter is given by the dashed lines in Fig. 12. The response shown was obtained by an iterative approach of adjusting the rotational position of the Möbius wire and the capacitive coupling of the input and output antennas. The passband is 90 MHz wide and is centered at 2.167 GHz, which corresponds to a 4.2% fractional bandwidth. The minimum insertion loss is 1 dB, and the return loss is 4 dB. Each of the two intrinsic transmission zeros is clearly visible. One is located just below the passband and the other is located slightly above the passband, which enhances the sharpness of the filter. Overall, the transfer function is very similar to that seen in some microstrip dual-mode ring-resonator bandpass filters [13]. A closer examination of the measured passband performance is given in Fig. 13. The phase response
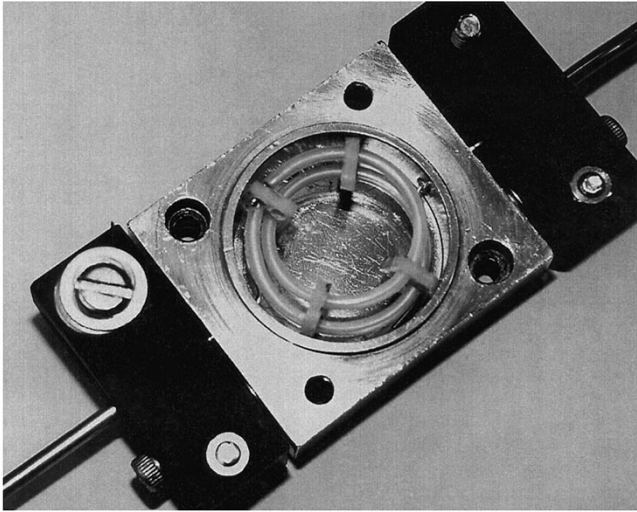
Fig. 11. A 4π Möbius wire in 2.5-cm-diameter copper cavity; 1.5-cm-long coupling antennas are bent in counterclockwise arcs to achieve proper capacitive coupling to the 4π Möbius wire.
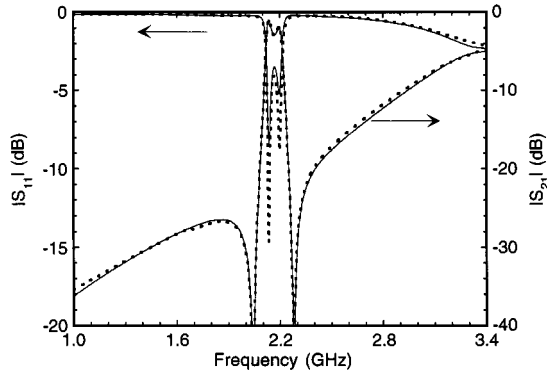

Fig. 12. The measured (dashed) and modeled (solid) magnitudes of the forward transmission ($|S_{21}|$) and reflection ($|S_{11}|$) scattering parameters of the 4π Möbius wire in 2.5-cm-diameter copper cavity shown in Fig. 12.
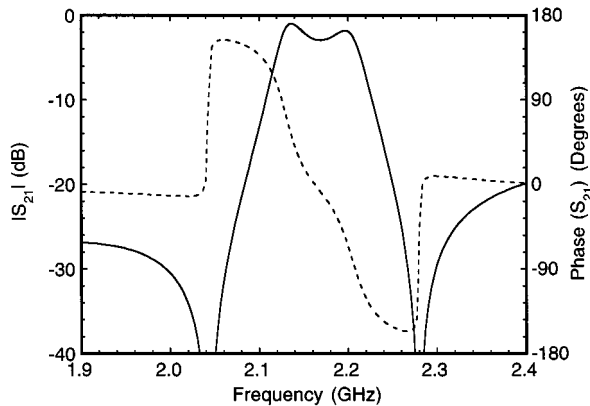

Fig. 13. Measured magnitude (solid) and phase (dashed) of the forward transmission scattering parameter of the device shown in Fig. 12. The phase has been corrected for the linear phase slope of the coaxial cables.

shown in Fig. 13 has been corrected for the linear phase slope of the input and output coaxial cables. A better transfer function could undoubtedly be obtained if tuning could be varied via feedthroughs in the cavity cover.
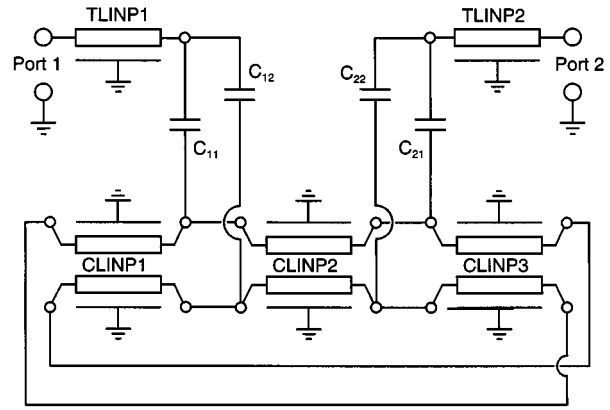

Fig. 14. Equivalent circuit for the 4π Möbius wire cavity resonator that gives the response shown by the solid lines in Fig. 13.

Although considerable work will be required to optimize passband performance and control out-of-band performance, the initial results are quite encouraging. Current plans are to fabricate a new cavity to facilitate tuning of the transfer characteristics. The data provided by this experiment have proven quite useful in the initial development of an equivalent circuit. The equivalent circuit response, shown by the solid lines in Fig. 12 and discussed in the next section, can be seen to be in good agreement with the measured data.

V. CIRCUIT MODEL

The equivalent circuit employed to model the measured filter response shown in Fig. 12 is shown in Fig. 14. The modeling was implemented using EESof version 6. Since the currents in the Möbius resonator closely resembles those of an odd mode on a pair of coupled lines, a coupled transmission-line model (CLINP1, CLINP2, and CLINP3) was chosen as the basic equivalent circuit element to model the Möbius wire-loaded cavity. The input and output transmission lines (TLINP1 and TLINP2) account for the input and output coaxial cables.

The other circuit elements required are those that describe the capacitive coupling between the input and output antennas and the Möbius wire resonator. To obtain the agreement between the measured (dashed lines) and modeled (solid lines) data shown in Fig. 12, it was necessary to allow the capacitive coupling elements (C_{11}, C_{12}, C_{21}, and C_{22}) to have both a frequency-independent term and a term that is linearly dependent with frequency ($C_{ij} = C_{0ij} + \omega C_{1ij}$). This is a reasonable method of accommodating, with a lumped element capacitance, the distributed nature of the capacitive coupling in the experiment.

It should be noted that the properties of all three coupled-line sections, except for their lengths, were identical. Since the geometric deformation of the wire was evenly distributed, no lumped element components are used to model the twist. This corroborates that the transmission zeroes are intrinsic to the circuit. To explore this concept further, the equivalent circuit was used to numerically investigate a loosely coupled resonator where all four coupling capacitances have been reduced by an identical factor. The total length of all three coupled-line sections was held constant so that their total electrical length at resonance (f_0) was 180°. Their relative lengths were varied to
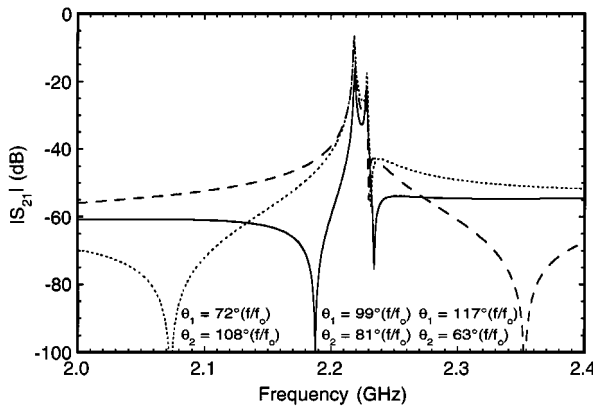
Fig. 15.   Predicted transmission zero location versus relative electrical length $(\theta_1 + \theta_2 = 180°$ at resonance, $f_0)$ using the conventions of Fig. 3.

study the behavior of the two transmission zeroes. As shown in Fig. 15, the behavior of the lower frequency transmission zero observed in Fig. 12 is consistent with the intrinsic transmission zero due to the short circuit at the output port. In contrast, the higher frequency transmission zero observed in Fig. 12 shows almost no change in frequency in Fig. 15, which is consistent with the intrinsic transmission zero due to the short circuit at the input port.

VI. CONCLUSION

Compact dual-mode resonators and bandpass filters have been realized by projecting a transmission line onto a nonorientable surface. The resulting geometry is analogous to a Möbius strip where the conductor defines the edge of the strip. This concept of employing a geometric deformation in order to contribute to the phase change required to achieve a resonance condition has resulted in a factor-of-four reduction in volume as compared to the equivalent conventional geometry. Both planar and wire-loaded cavity implementations have been demonstrated. Higher order structures capable of a factor-of-16 reduction in volume have been presented. It was shown that these structures possess intrinsic transmission zeros, which can greatly aid in obtaining desirable bandpass filter characteristics. An equivalent circuit was introduced, which demonstrated excellent agreement with the measured data.

Future effort will be focused on addressing issues of tuning, coupling, and harmonic suppression. Of particular interest is the integration of dielectric loading with Möbius wire-loaded cavity resonators. More advanced resonators involving more complicated geometries are also being pursued. The possibility of exploiting other topological geometries for microwave filter applications is being investigated.

REFERENCES

[1] J. M. Pond, "Möbius filters and resonators," in *2000 IEEE Int. Microwave Symp. Dig.*, vol. 3, June 2000, pp. 1653–1656.
[2] *Webster's New Collegiate Dictionary*.   Springfield, MA: G.&C. Merriam , 1974.
[3] W. Lietzmann, *Visual Topology*.   New York: Elsevier, 1965.
[4] J. S. Carter, *How Surfaces Intersect in Space: An Introduction to Topology*, 2nd ed.   Singapore: World Scientific, 1995.
[5] W. V. Tyminski and A. E. Hylas, "A wide-band hybrid ring for UHF," *Proc. IRE*, vol. 41, pp. 81–87, Jan. 1953.
[6] D. Rubin and D. Saul, "mm wave MIC's use low value dielectric substrates," *Microwave J.*, vol. 19, no. 11, pp. 35–39, Nov. 1976.
[7] B. R. Heimer, L. Fan, and K. Chang, "Uniplanar hybrid couplers using asymmetrical coplanar striplines," *IEEE Trans. Microwave Theory Tech.*, vol. 45, no. 12, pp. 2234–2240, Dec. 1997.
[8] B.-H. Margulescu, E. Moisan, P. Legaud, E. Panard, and I. Zaquine, "New wideband, 0.67 λ_g circumference 180° hybrid ring coupler," *Electron. Lett.*, vol. 330, no. 4, pp. 299–300, Feb. 1994.
[9] H.-R. Ahn, I. Wolff, and I.-S. Chang, "Termination impedances, power division, and ring hybrids," *IEEE Trans. Microwave Theory Tech.*, vol. 45, pp. 2241–2247, Dec. 1997.
[10] K. Chang, *Microwave Ring Circuits and Antennas*.   New York: John Wiley and Sons, Inc., 1996.
[11] J. Wested and E. Andersen, "Resonance splitting in nonuniform ring resonators," *Electron. Lett.*, vol. 8, no. 12, pp. 301–302, June 1972.
[12] U. Karacaoglu, I. D. Robertson, and M. Guglielmi, "A dual-mode microstrip ring resonator filter with active devices for loss compensation," in *1993 IEEE Int. Microwave Symp. Dig.*, vol. 1, June 1993, pp. 189–192.
[13] U. Karacaoglu, D. Sanchez-Hernandez, I. D. Robertson, and M. Guglielmi, "Harmonic suppression in microstrip dual-mode ring-resonator bandpass filters," in *1996 IEEE Int. Microwave Symp. Dig.*, vol. 3, June 1996, pp. 1635–1638.
[14] W. W. Macalpine and R. O. Schildknecht, "Coaxial resonators with helical inner conductor," *Proc. IRE*, vol. 47, pp. 2099–2105, Dec. 1959.
[15] S. J. Fiedziuszko and R. S. Kwok, "Novel helical resonator filter structures," in *1998 IEEE Int. Microwave Symp. Dig.*, vol. 3, June 1998, pp. 1323–1326.

Jeffrey M. Pond, photograph and biography not available at the time of publication.